E3S Web of Conferences **439**, 02007 (2023) https://doi.org/10.1051/e3sconf/202343902007
EBGBM 2023

Study on Seismic Performance of Cold-Formed Thin-Walled Steel-Straw Board Composite Wall with Diagonal Brace

Linjun Li[a*], Jinsong Lei[b]

Southwest University of Science and Technology (Mianyang) College of Civil Engineering and Architecture, Mianyang China 621010

Abstract: The composite wall studied in this paper is based on the original cold-formed thin-walled steel-straw board composite wall, which is set up with inclined braces and rigid inclined braces to improve its seismic performance. The factors of aspect ratio are analyzed, and the formula of shear bearing capacity of composite wall is deduced. The results show that: (1) When the height-width ratio of the composite wall is 2.4m×1.2m, 1.8m×1.2m and 1.2m×1.2m respectively, the yield strength of the composite wall is 35.78kN, 37.47kN and 54.23kN respectively. The yield strength of the former increases by 4.72 %, and the yield strength of the latter increases by 44.73 %. (2) Using the effective strip method, the error of the derived shear capacity formula is not large, and the difference between the experimental value and the simulated value is not large, in order to provide some reference for the seismic design of this kind of cold-formed thin-walled steel-strawboard composite wall with diagonal brace.

1 Introduction

Gao Wancheng[3] summarized the shear test results of cold-formed thin-walled steel walls at home and abroad, and gave the influence of wall panel type, wall height-width ratio, opening and loading mode on the shear capacity of the wall. In terms of numerical simulation: Nie Shaofeng[8,9] derived the calculation method of the shear capacity of the wall by using the overall analysis method and the shear flow method respectively, and the calculation formula is biased towards safety. Niari[1] used ABAQUS software to simulate the wall of thin steel plate. In the model, all components were simulated by shell elements, and the self-tapping screws were simulated by nonlinear connection elements. The contact between the components was considered and the geometric nonlinearity was turned on.

Based on the previous research, ABAQUS is used to analyze the influence of the change of height-width ratio parameters on the seismic performance of the composite wall with diagonal bracing under horizontal monotonic load, and a simplified model of wall bearing capacity is established to derive the formula, which provides a theoretical reference for such engineering applications.

2 Establishment of finite element model

2.1 ABAQUS selection

This section will introduce the finite element analysis software ABAQUS6.14 in detail, and establish a new type of cold-formed thin-walled steel composite wall with diagonal brace.

2.1.2 Model unit selection and meshing

The light steel keel consists of steel column, diagonal brace, upper guide rail and lower guide rail connected by self-tapping screws. Q235 galvanized cold-formed thin-walled C steel is used for the steel column and diagonal bracing of the light steel keel. The specifications are C90x40x15x1mm (web height x flange width x curling width x section thickness). Because the side column of the wall specimen is subjected to a large force under the action of earthquake, the side column is connected by two back-to-back C-shaped steel columns through self-tapping screws; the middle column is located in the middle of the wall; the self-tapping screw used in the production process of light steel keel is ST3.5x75 mm plum blossom countersunk head self-tapping screw; the upper and lower guide rails adopt Q235 galvanized cold-formed thin-walled U-shaped steel with a specification of U93x45x1.5mm (web height x flange width x cross-section thickness), and are

Corresponding author: [a*]1240864314@ qq.ccom, [b]173266820@ qq.ccom

 https://doi.org/10.1051/e3sconf/202343902007

connected to the top beam and the bottom beam through M18 high-strength 10.9 bolts. The section of the keel column and the guide rail is shown in Figure 1.

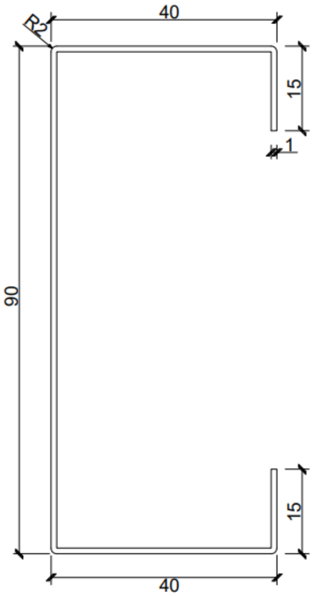

(a) Columns, bracings, cross bracings

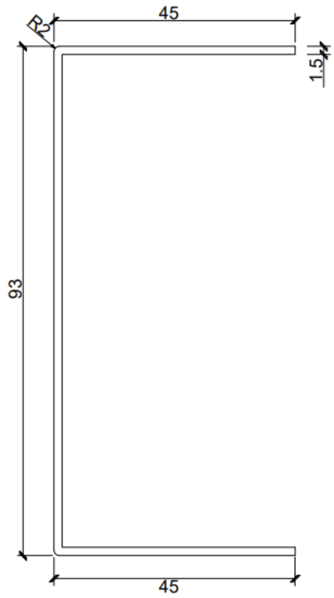

(b) Upper guide rail, lower guide rail

Figure 1 Cross-section of keel column and guide rail

2.1.3 Simulation method of self-tapping screw connection

The simulation of the self-tapping screw is based on the Cartesian and aline connectors in Basic to simulate the connection of the self-tapping screw between the straw board and the light steel skeleton, as shown in Figures 2 and 3.

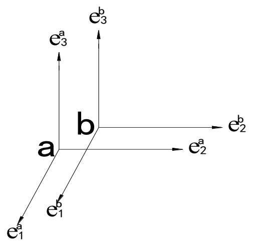

Figure 2 Cartesiana type unit

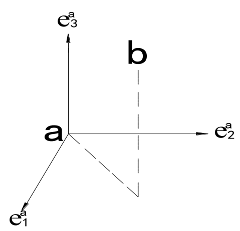

Figure 3 Alinc type unit

2.1.4 Loading method and boundary conditions

The translational degrees of freedom of the guide rail in all directions under the wall are constrained, that is, U1 = U2 = U3 = 0. The translational degrees of freedom of the guide rail web along the out-of-plane direction and the rotational degrees of freedom outside the steering plane are constrained, that is, U1 = UR2 = UR3 = 0. At the same time, in order to facilitate the result query and data extraction of finite element simulation, a reference point RP-1 is established outside the wall model during modeling, and RP-1 is used as a control point to couple with the top beam web of the wall, as shown in Figs.4 and 5.

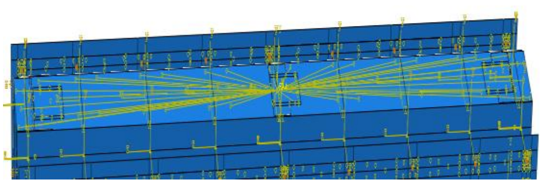

Figure 4 Coupling relationship between top beam web and reference point RP-1

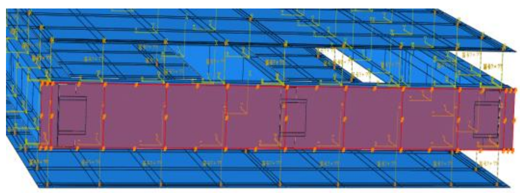

Figure 5 Boundary conditions of the bottom beam

3 Model validation in this paper

The finite element analysis software ABAQUS is used to simulate and analyze the sdwgc cold-formed thin-walled steel wall in reference[12]. The finite element analysis and test results are compared and verified from three aspects: failure mode, skeleton curve and eigenvalue.

Table 1 Parameters of each component of the internal non-diagonal brace composite wall

test piece	Wall size	thickness of post	thickness of plating	strength of column	vertical load	prop spacing	screw spacing (mm)	
	(m)	(mm)	(mm)	(MPa)	(KN)	(mm)	edge	interior
1	1.2×2.4	1	58	235	30	600	150	300

3.1 Comparison of failure modes

The specimen is a composite wall specimen without internal bracing. During the loading process, local buckling occurs at the bottom of the side column, and the wrinkles of the straw board are mainly concentrated around the wallboard. Figure 6 is the finite element failure mode, which is basically consistent with the failure phenomenon of the reference test.

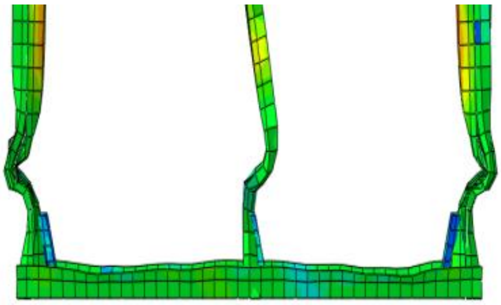

Figure 6 Finite element failure pattern

3.2 Comparison of skeleton curves

The skeleton curve[11] refers to the curve formed by connecting the peak points reached in each displacement cycle from the initial point of loading. The curve can reflect the stress and ductility of the member at different stages. The comparison results are shown in Figure 7.

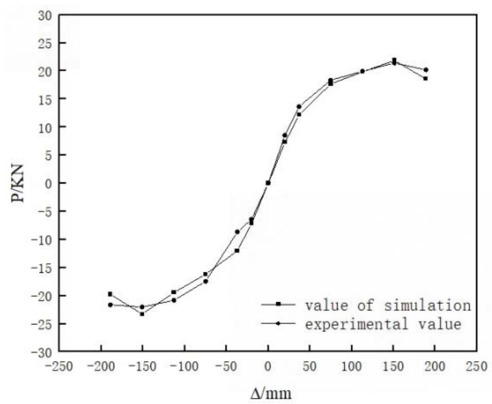

Figure 7 Simulated skeleton curve and experimental comparison chart

It can be seen from Fig.7 that the skeleton curves are in good agreement, but the peak load of the finite element simulation is slightly higher than the peak load of the test. Because the finite element simulation model is a simplified model, the results are not completely consistent.

3.3 Comparison of eigenvalues

From the skeleton curve of the model, the yield displacement, yield load and peak load of the model can be analyzed. In this paper, the Park method is used, see figure 8.

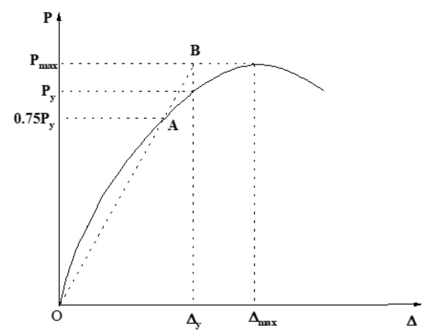

Figure 8 Park method to determine the yield point.

In addition, the maximum load P_{max} and maximum displacement Δ_{max} of the specimen correspond to the peak point in the skeleton curve, and the data are shown in Table 1.

Table 2 Comparison of finite element and test eigenvalues

test piece	yield load/KN			yield displacement/mm			maximum load/KN		
	experiment	finite element	error	experiment	finite element	error	experiment	finite element	error
No bracing	18.90	18.43	2.49%	80.80	87.99	8.90%	21.41	21.86	2.10%

It can be seen from Table 2, the error between the finite element and the test is small and the agreement is good, indicating that the finite element model is reasonable and can be used for further parameter analysis.

4 Finite element analysis of seismic performance of composite wall

On the basis of verifying the model, Abaqus was used to change the support mode in the wall, and the influence of relevant parameters on the seismic performance of the composite wall was analyzed, and the characteristic values of bearing capacity were compared. It is found that the seismic performance of the composite wall with diagonal brace is better than the former two.

4.1 Analysis of the influence of support mode

The composite wall model of horizontal brace and diagonal brace is established and compared with the original. The support adopts Q235 steel (C90x40x15x1mm). Except for different support methods, other parameters are the same. The stress nephogram and skeleton curve of the wall are shown in figure 9 below:

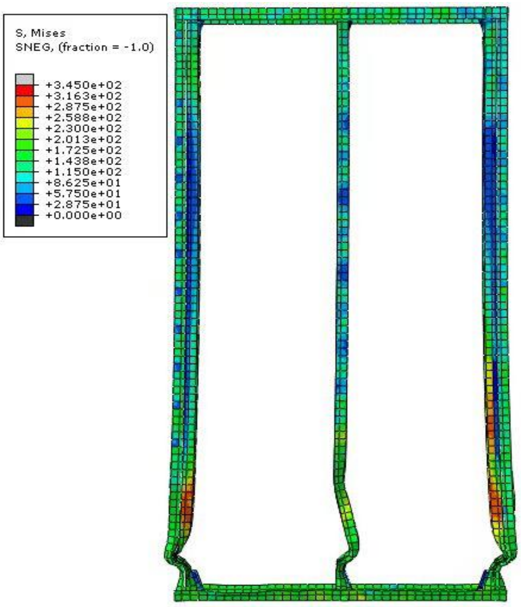

(a) Internal non-transverse support wall skeleton stress cloud diagram

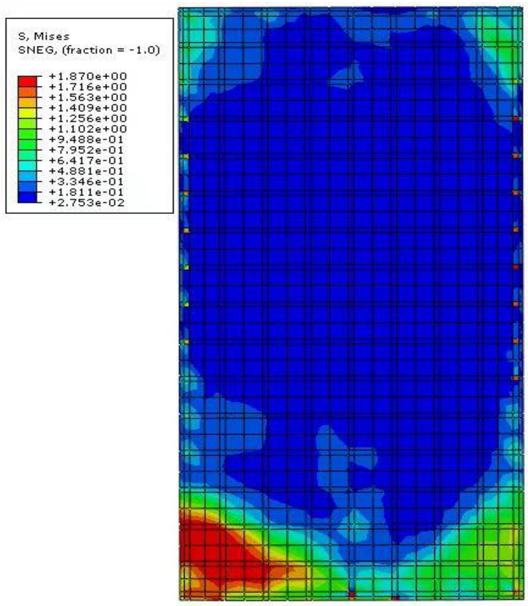

(b) Internal no transverse support wall panel stress cloud diagram

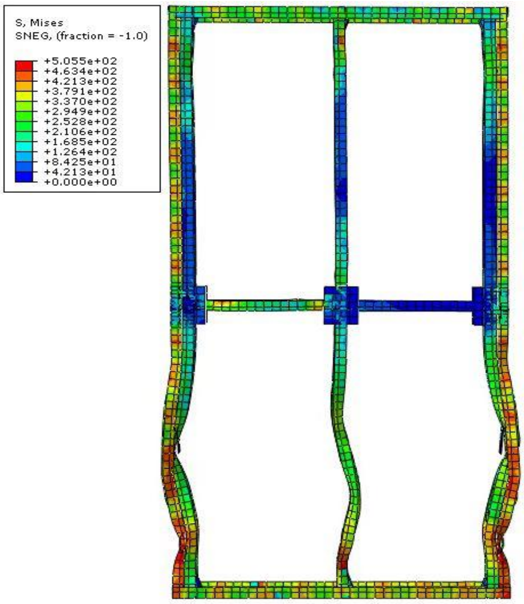

(c) The stress cloud diagram of the inner cross-bracing wall skeleton

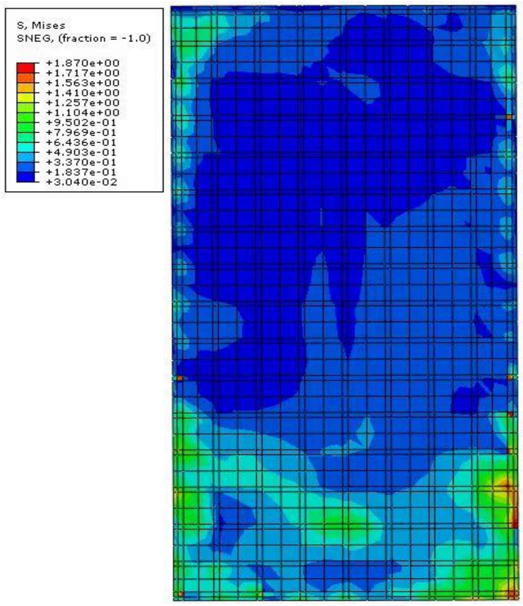

(d) The stress cloud diagram of the wall panel with horizontal braces inside

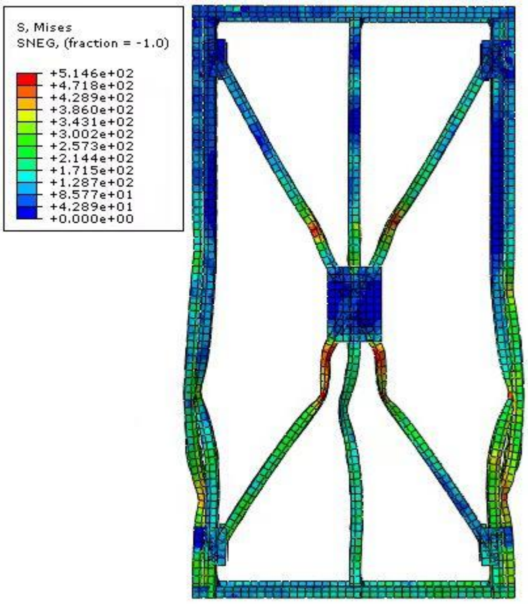

(e) Stress cloud diagram of internal bracing wall skeleton

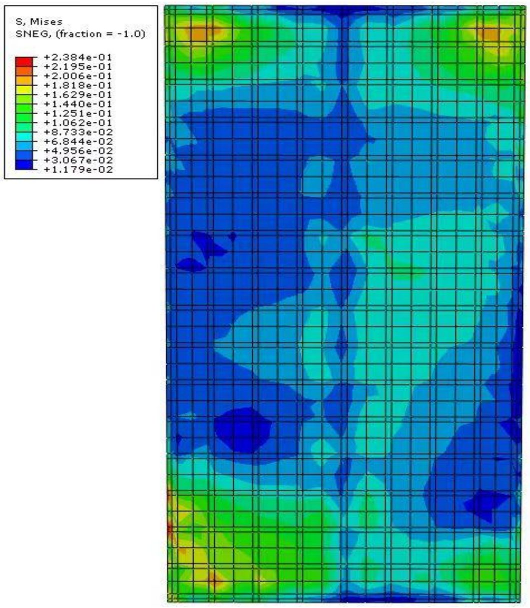

(f) Stress cloud diagram of internal bracing wall panel

Figure 9 Varying stress cloud diagram of different support methods

It can be seen from Fig.9 that the composite wall with inclined support can make full use of the steel performance before the end of loading, and the stress is concentrated in the middle of the support of the composite wall.

4.1.1 Skeleton curve and its eigenvalue comparison

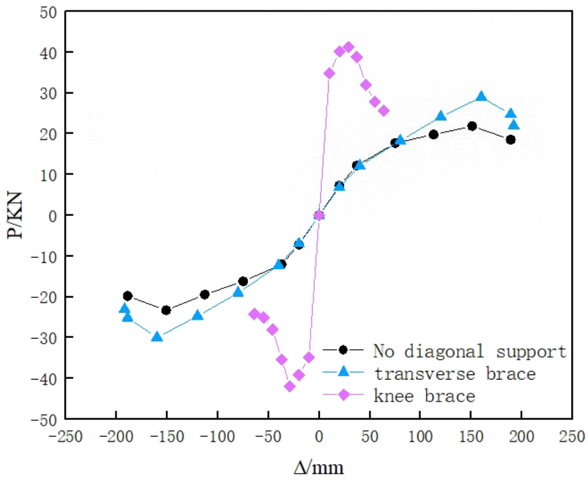

Figure 10 Comparison diagram of skeleton curve of wall with different support methods

The skeleton curve can reflect the yield displacement, yield load, peak point and ductility coefficient of the component. The calculation of ductility is in accordance with the provisions of the " Building Seismic Test Procedures "[11], and the ductility coefficient is used to represent the ductility. The calculation formula is shown in (1). In the formula, the ultimate displacement needs to be determined, and the ultimate displacement is specified as the displacement corresponding to 0.85 P_{max} in the descending section of the skeleton curve.

$$\mu = \frac{\Delta_u}{\Delta_y} \tag{1}$$

In the formula: Δ_u is the ultimate displacement of the specimen;

Δ_y is the peak displacement corresponding to the peak load of the specimen.

The skeleton curve of the composite wall is shown in Fig.10, and the corresponding seismic bearing capacity characteristic value is shown in Table 3. According to the relevant regulations, when the ductility coefficient is less than or equal to 1.5, the deformation capacity of the specimen is considered to be weak. When the ductility coefficient is greater than 3.5, it is considered that the deformation capacity of the specimen is superior; when the deformation coefficient is in the middle value, the deformation ability of the specimen is considered to be medium.

Table 3 Comparison of bearing capacity characteristic values of walls with different support methods

supporting way	yield displacement/mm	yield load/ KN	peak load/ KN	ductility factor
No diagonal support	87.99	18.43	21.86	2.15
transverse brace	137.89	26.30	28.97	2.37
knee brace	11.87	35.78	41.28	3.53

The results show that the seismic performance of the supported model is better than that of the original model, and the improvement of the internal bracing is the most obvious. The yield load, peak load and continuation coefficient are increased by 94.14%, 88.84% and 64.19% respectively, indicating that the composite wall with rigid bracing can effectively improve the seismic performance.

5 The influence of parameter changes on the composite wall

5.1 Effect of aspect ratio on the bearing capacity of the wall

5.1.1 Comparison of failure modes

The parameter analysis of the composite wall is carried out by numerical simulation, and the influence of changing the aspect ratio on the bearing capacity of the composite wall is considered. The parameters of each reference are shown in Table 4.

Table 4 Parameters of each datum under different height and width ratio composite walls

test piece	Wall size	Column wall thickness	strength of column	prop spacing	screw spacing(mm)	
	(m)	(mm)	(MPa)	(mm)	edge	interior
1	1.8×1.2	1	235	600	150	300
2	2.4×1.2	1	235	600	150	300
3	1.2×1.2	1	235	600	150	300

After the finite element simulation analysis, the stress cloud diagram of each component of the composite wall can be seen in figure 11 through post-processing.

 https://doi.org/10.1051/e3sconf/202343902007

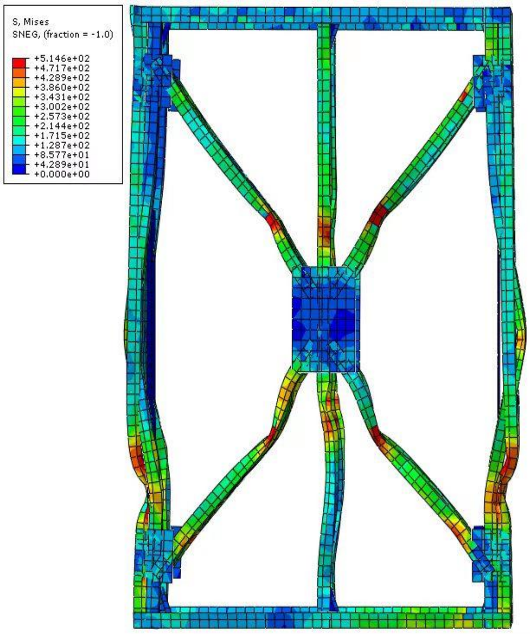

(a) 1.8m×1.2m wall skeleton stress nephogram

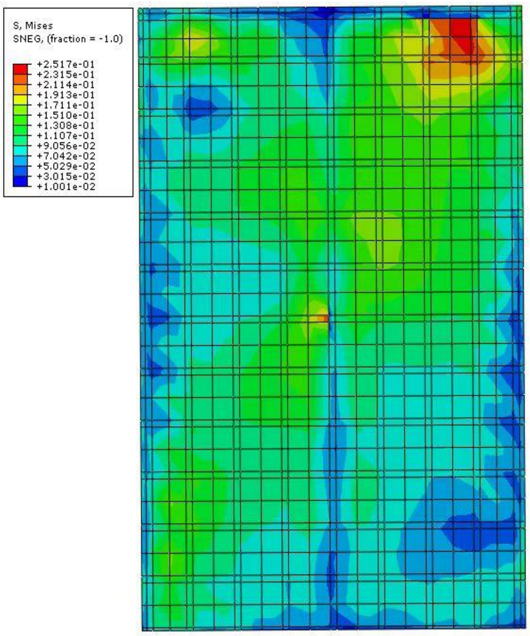

(b) 1.8m×1.2m wall panel stress nephogram

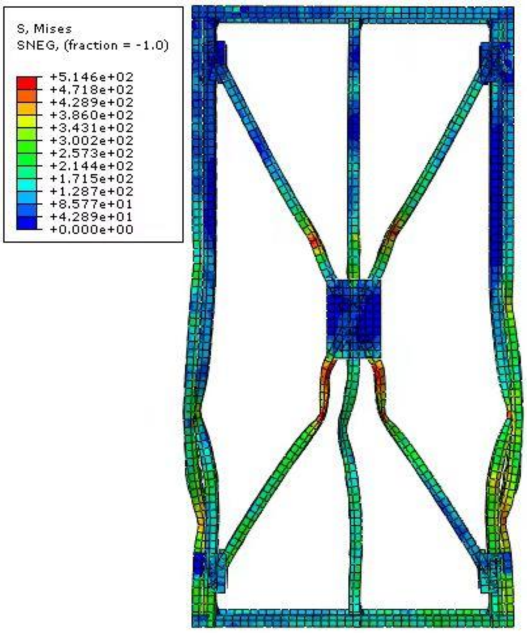

(c) 2.4m×1.2m wall skeleton stress nephogram

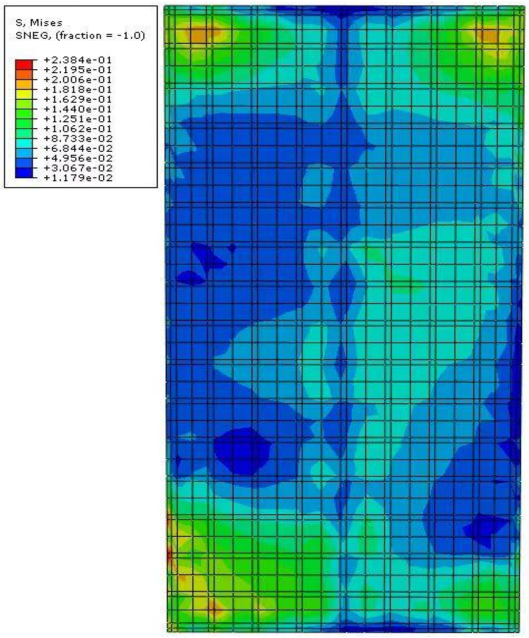

(d) 2.4m×1.2m wall panel stress nephogram

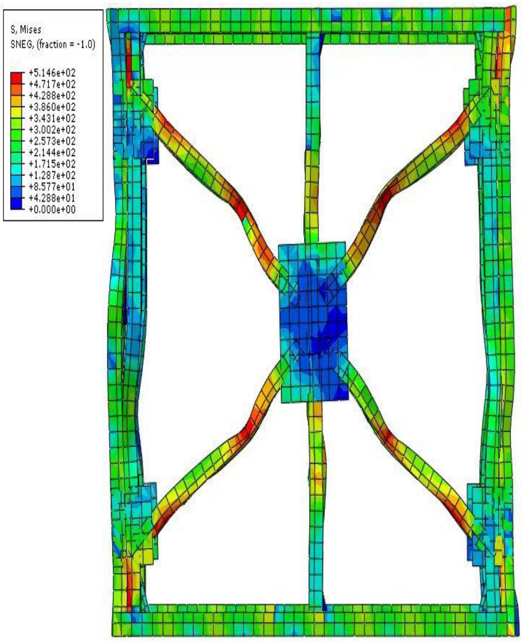

(e) 1.2m×1.2m wall skeleton stress nephogram

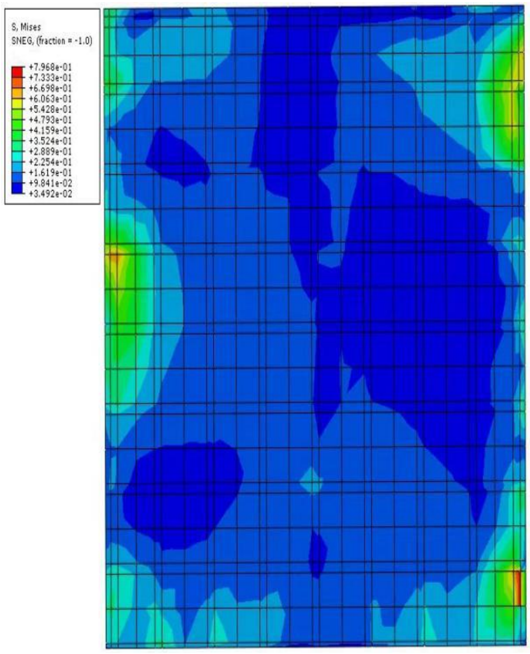

(f) 1.2m×1.2m wall panel stress nephogram

Figure 11 Stress cloud diagram of different aspect ratio composite wall

It can be seen from Fig.11 that the columns and braces of the composite wall are buckling, and the most serious is the 2.4m×1.2m composite wall. It can be seen from the figure that the stress of the braces and columns decreases with the decrease of the height-span ratio, that is, the damage of the composite wall is weakened. This is because most of the force of the composite wall is borne by the skeleton and brace of the composite wall.

5.1.2 Skeleton curve and eigenvalue comparison

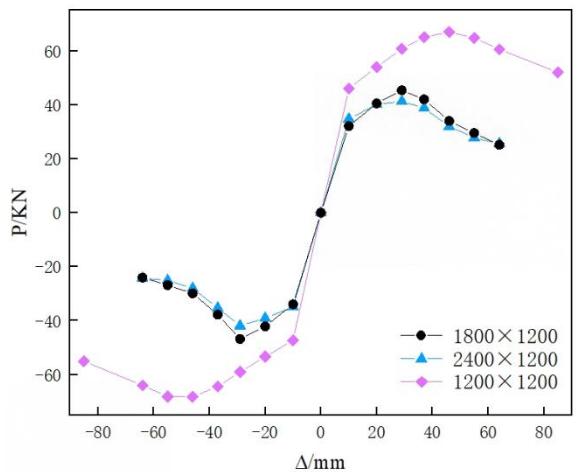

Figure 12 Comparison diagram of skeleton curve of different height and width ratio composite walls

Table 5 Comparison of seismic bearing capacity characteristic values of different aspect ratio composite walls

Wall size/(m)	yield load/KN	Yield displacement /mm	peak load/KN	ductility factor
1.8×1.2	37.47	16.39	45.36	2.50
2.4×1.2	35.78	11.87	41.28	3.53
1.2×1.2	54.23	20.31	66.96	3.59

It can be seen from Fig.12 and Table 5 that reducing the height-span ratio can improve the seismic performance of the composite wall, because it can improve the comprehensive force of the column and the diagonal brace and reduce the overall deformation of the composite wall.

6 Calculation formula of shear bearing capacity of composite wall

The theoretical formula of shear bearing capacity of cold-formed thin-walled steel-strawboard composite wall with diagonal brace is derived. In order to understand the failure mode of composite wall, the corresponding balance formula is established based on the failure model of wall, so as to obtain the calculation method of bearing capacity.

6.1 Effective Strip Method

Summarizing the domestic and foreign literature[14,4,2,5,7,10], it is concluded that the failure modes of the composite wall mainly include the following situations : shear failure of the self-tapping screw, failure of the self-tapping screw to pull out the covering panel, failure of the wall panel, buckling failure of the diagonal brace, etc. According to the North American AISI specification, the formula for calculating the strength of screw connections is as follows:

(1) When $\frac{t_2}{t_1} \le 1$, P_{ns} should take the minimum value of the three formulas:

Anti-tilt strength of screw:

$$P_{ns} = 4.2\sqrt{t_2^3 d} \cdot F_{u2} \quad (2)$$

The strength determined by the covering panel:

$$P_{ns} = 2.7 t_1 d F_{u1} \quad (3)$$

Strength determined by light steel skeleton:

$$P_{ns} = 2.7 t_2 d F_{u1} \quad (4)$$

(2) When $\frac{t_2}{t_1} \geq 2.5$, P_{ns} should take the minimum value of the two formulas.

$$P_{ns} = 2.7 t_1 d F_{u1} \quad (5)$$

$$P_{ns} = 2.7 t_2 d F_{u2} \quad (6)$$

(3) When $1 \leq \frac{t_2}{t_1} \leq 2.5$, P_{ns} should take the linear interpolation of the above two cases.

Of which:

t_1 —the thickness of the cladding panel;

t_2 —The thickness of light steel skeleton;

d —The diameter of the screw;

F_{u1} —the tensile strength of the cladding panel;

F_{u2} —Tensile strength of light steel skeleton.

Foreign scholars deduced the calculation formula of shear capacity of composite wall with thin steel plate by effective strip method, and the stress model is shown in Fig.13. $V_n = T_n \cdot \alpha$, of which T_n is determined by the minimum value of the connection strength of the screw and the bearing capacity of the wall panel, that is, the following formula :

$$T_n = \min\left(\sum_i^n P_{ns,i}, W_e T_{sh} F_y\right) \quad (7)$$

Of which:

P_{ns} —The minimum value of the screw connection strength is obtained from Eqs. (2) - (6). The force analysis of the screw is shown in Fig.14.

T —Steel plate thickness;

F_y —Yield load of steel plate;

W_e —Effective band width.

$$W_e = \begin{cases} W_{\max} & (\lambda \leq 0.0819) \\ \rho W_{\max} & (\lambda \geq 0.0819) \end{cases} \quad (8)$$

$$\rho = \frac{1 - 0.55(\lambda - 0.0819)^{0.12}}{\lambda^{0.12}} \quad (9)$$

$$\lambda = \frac{1.736\alpha_1\alpha_2}{\beta_1\beta_2\beta_3\alpha} \quad (10)$$

Of which:

$$\alpha_1 = \frac{F_{ush}}{310.3}, \alpha_2 = \frac{F_{uf}}{310.3}, \beta_1 = \frac{t_{sh}}{0.457},$$

$$\beta_2 = \frac{t_f}{0.457}, \beta_3 = \frac{s}{152.4} \quad (11)$$

F_{ush} —Tensile strength of steel plate;

F_{uf} —The smaller value of the tensile strength of the wall frame column and the top and bottom guide beams;

t_{sh} —Thickness of the steel plate;

t_f —The smaller value of the wall thickness of the wall frame column and the top and bottom guide beams;

S —Screw spacing.

The formula of shear bearing capacity of composite wall is derived by using effective strip method:

$$P_{wall} = \min\left\{\left(\frac{W_e \cdot P_{ns,t}}{2s \cdot \sin\alpha} + \frac{W_e \cdot P_{ns,s}}{2\cos\alpha} + P_{ns,t\xi s}\right) \cdot \cos\alpha, W_e t F_y \cos\alpha\right\} \quad (12)$$

Of which:

$P_{ns,t}$ —The connection strength between the wall panel and the top and bottom guide beams;

$P_{ns,s}$ —The connection strength between wall panel and wall frame column;

$P_{ns,t\xi s}$ —The connection strength between the wall panel and the guide beam and the wall column.

The relationship between the arrangement of screws and the maximum effective width is shown in Fig.15.

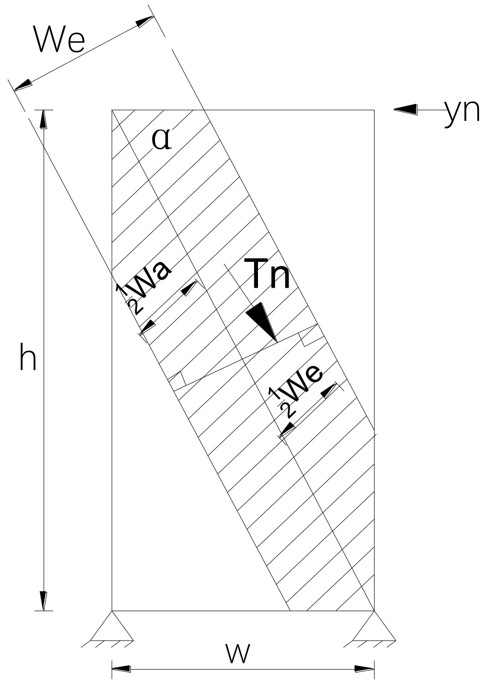

Figure 13 Force analysis diagram of effective strip method model

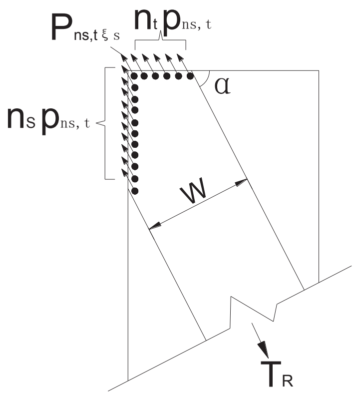

Figure 14 Screw force analysis diagram

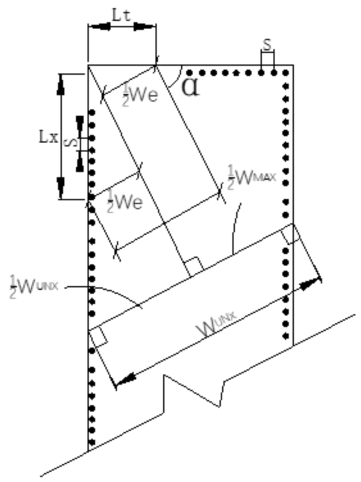

Figure 15 Schematic diagram of screw arrangement and maximum effective width

6.2 Comparison of finite element simulation results and overall analysis results

The calculated value of the shear bearing capacity of the composite wall derived by the effective strip method is compared with the finite element simulation results.

The data of three different composite walls with diagonal bracings with wall sizes of 2.4m×1.2m, 1.8m×1.2m and 1.2m×1.2m were compared with the shear bearing capacity formula derived from the effective strip method abroad, and then summarized and analyzed.

Comparison process:

(1) The finite element simulation data of composite wall with diagonal bracings with wall size of 2.4m×1.2m are compared with the effective strip method formula.

1. Calculation of maximum effective strip width

$$F_{ush} = 1.87MPa \quad t_{sh} = 58mm$$

$$F_{uf} = 344.70MPa \quad t_f = 1mm$$

$$\tan\alpha = \frac{2400}{1200} = 2 \qquad \alpha = \arctan 2 = 63.43^\circ$$

$$W_{\max} = \frac{W}{\sin\alpha} = \frac{1200}{\sin 63.43^\circ} = 1341.70\,mm$$

2. Effective strip width calculation

$$\alpha_1 = \frac{F_{ush}}{310.3} = 0.006 \quad \alpha_2 = \frac{F_{uf}}{310.3} = 1.111$$

$$\beta_1 = \frac{t_{sh}}{0.457} = 126.92$$

$$\beta_2 = \frac{t_f}{0.457} = 2.19$$

$$\beta_3 = \frac{s}{152.4} = 0.98$$

Get:

$$\lambda = \frac{1.736\alpha_1\alpha_2}{\beta_1\beta_2\beta_3} = \frac{1.736\times0.006\times1.111}{126.92\times2.19\times0.98} = 0.0000425,$$

$$\lambda \le 0.0819$$

So: $W_e = W_{\max} = 1341.70\,mm$

3. Screw shear strength value calculation

According to the simulation data, it can be seen that the strength of the screw connection is determined by the light steel skeleton. The strength of the screw connection is 4.467KN calculated by the formula.

Get: $P_{ns,t} = P_{ns,s} = P_{ns,t\zeta s} = 4.467KN$

4. Calculation of shear bearing capacity of composite wall

$$P_{wall} = \min\left\{\left(\frac{W_e\cdot P_{ns,t}}{2s\cdot\sin\alpha} + \frac{W_e\cdot P_{ns,s}}{2s\cdot\cos\alpha} + P_{ns,t\xi s}\right)\cdot\cos\alpha, W_e t F_y\cos\alpha\right\}$$

The shear bearing capacity of the composite wall is derived from the strength value of the self-tapping screw connection:

$$\left(\frac{W_e\cdot P_{ns,t}}{2s\cdot\sin\alpha} + \frac{W_e\cdot P_{ns,s}}{2s\cdot\cos\alpha} + P_{ns,t\xi s}\right)\cdot\cos\alpha = 31.97KN$$

The shear bearing capacity of the composite wall is deduced from the tensile strength value of the straw board:

$$W_e t F_y\cos\alpha = 65.09\,KN$$

$$P_{wall} = 31.97KN$$

Therefore, the smaller value between the two, that is, 31.97KN, is taken as the shear capacity of the composite wall.

(2) The finite element simulation data of 1.8m × 1.2m composite wall with diagonal bracing are compared with the formula of effective strip method.

Similar to the above solution process, not too much calculation is done here, only the calculation results are given.

The shear bearing capacity of the composite wall is derived from the strength value of the self-tapping screw connection:

$$\left(\frac{W_e\cdot P_{ns,t}}{2s\cdot\sin\alpha} + \frac{W_e\cdot P_{ns,s}}{2s\cdot\cos\alpha} + P_{ns,t\xi s}\right)\cdot\cos\alpha = 38.27KN$$

The shear bearing capacity of the composite wall is deduced from the tensile strength value of the straw board:

$$W_e t F_y\cos\alpha = 69.97KN$$

$$P_{wall} = 38.27KN$$

Therefore, the smaller value between the two, that is, 38.27KN, is taken as the shear capacity of the composite wall.

(3) The finite element simulation data of 1.2m×1.2m composite wall with diagonal bracing are compared with the formula of effective strip method.

Similar to the above solution process, not too much calculation is done here, only the calculation results are given.

The shear bearing capacity of the composite wall is derived from the strength value of the self-tapping screw connection:

$$\left(\frac{W_e \cdot P_{ns,t}}{2s \cdot \sin\alpha} + \frac{W_e \cdot P_{ns,s}}{2s \cdot \cos\alpha} + P_{ns,t\xi s}\right) \cdot \cos\alpha = 53.70KN$$

The shear bearing capacity of the composite wall is deduced from the tensile strength value of the straw board:

$$W_e t F_y \cos\alpha = 82.33KN$$

$$P_{wall} = 53.70KN$$

Therefore, the smaller value between the two, that is, 53.70KN, is taken as the shear capacity of the composite wall.

Table 6 Comparison of simulation results and theoretical calculation results of composite walls with different high span ratios

Wall size/m	theoretical yield load/kN	Simulating yield load/kN	error/%
2.4×1.2	31.97	35.78	10.66
1.8×1.2	38.27	37.47	2.09
1.2×1.2	53.70	53.23	0.99

It can be seen from Table 6 that the minimum error between the theoretical calculation results and the test results is 0.99 %, and the maximum is 10.66 %. It shows that the formula derived from the effective strip method is reasonable and can provide reference for engineering design.

6.3 The experimental results are compared with the results of the effective strip method.

In order to further verify the correctness of the shear bearing capacity formula of the composite wall derived by the effective strip method, this paper not only quotes the data in Zhang Enyuan 's[13] paper, that is, Sddg1.0ic and Sdsg1.0ic test data, but also quotes the data of Ling Ligai 's[6] paper, that is, wsS-so75-0.75-1 specimen data. The parameters are substituted into the shear capacity formula of the composite wall derived by the effective strip method, and the comparison results are shown in table 7.

Table 7 Comparison of test results and theoretical calculation results

Wall size/m	Wall panel thickness/mm	thickness of post/mm	board strength/MPa	strength of column/MPa	computation/KN	test result/KN	error/%
2.4×1.2	1	1	235	235	20.68	23.70	14.6
2.4×1.2	2	1	235	235	41.37	39.29	5.29
3.0×2.4	0.42	0.75	550	550	29.27	29.83	0.19

It can be seen from Table 7 that the error is controlled within 15%, which is in good agreement. The surface test value can also be in good agreement with the shear capacity formula of the composite wall derived from the effective strip method, which further verifies the correctness and wide applicability of the effective strip method.

7 Conclusion

In order to be better applied to the composite wall, the finite element simulation analysis and theoretical derivation analysis of the seismic performance of the cold-formed thin-walled steel-straw board composite wall with diagonal bracing are carried out in this paper. The influence factors of height-width ratio on the bearing capacity of composite wall under low cyclic horizontal load were studied. The effective slice method for calculating the shear capacity of composite walls is introduced, and its correctness and wide applicability are verified. Based on this, the following conclusions can be drawn:

(1) Based on the test results of the existing literature, the finite element analysis of the cold-formed thin-walled steel-strawboard composite wall with diagonal braces under low-cycle reciprocating horizontal loading was carried out by using ABAQUS software. The results show that the error between the maximum load value of the experiment and the maximum load value of the finite element simulation is 2.10 %, the error of the yield load is 2.49 %, and the error of the yield displacement is 8.90 %. It can be seen that the finite element simulation values are in good agreement with the experimental values, which verifies the correctness and rationality of the finite element model.

(2) When the aspect ratio of the composite wall is 2.4m×1.2m, 1.8m×1.2m and 1.2m×1.2m respectively, the yield strength of the former increases by 4.72%, and the yield strength of the latter increases by 44.73%.

(3) Through the parameter analysis of the finite element model, it can be seen that the aspect ratio will affect the bearing capacity of the wall. Reducing the aspect ratio can improve the bearing capacity of the wall, but the aspect ratio should not be less than 1.

(4) In this paper, the effective strip method is used to derive the calculation formula of the shear capacity of the composite wall. The minimum error between the theoretical calculation result and the test result is 0.99 %, and the maximum is 10.66 %. The subsequent comparison can be well consistent with the test value and the simulated value.

References

1. Shirin, E. N. and R. Behzad, et al. (2015). "Seismic behavior of steel sheathed cold-formed steel shear wall: Experimental investigation and numerical modeling." Thin-Walled Structures 96.
2. Fu Zhengbing (2012). shear capacity analysis of cold-formed thin-walled steel structure residential composite wall, Hefei University of Technology. Master: 73.
3. Gao Wancheng and Xiao Yan (2014). "A Review of Shear Behavior of Cold-formed Thin-walled Steel Composite Walls." Architectural Structure Journal 35 (04) : 30-40.
4. GUO Peng and HE Baokang et al. (2007). A review of the shear behavior of cold-formed steel column composite walls. The 7th National Symposium on Modern Structural Engineering. Hangzhou, Zhejiang, China: 8.
5. Li Yuanqi and Liu Fei et al. (2012). "Experimental study on seismic performance of S350 cold-formed thin-walled steel keel composite wall." Journal of Civil Engineering 45 (12) : 83-90.
6. Ling (2008). experimental study on shear performance of high strength cold-formed thin-walled steel column single-sided composite wall, Xi 'an University of Architecture and Technology.Master : 70.
7. Liu Bin and Hao Jiping (2015). "Experimental study on shear behavior of sprayed lightweight mortar-cold-formed thin-walled steel composite wall." Journal of Civil Engineering 48 (04) : 31-41.
8. Nie Shaofeng and Zhou Tianhua et al. (2007). "Research on simplified calculation method of shear capacity of cold-formed steel composite wall." Journal of Xi 'an University of Architecture and Technology (Natural Science Edition) (05): 598-604.
9. Nie Shaofeng and Zhou Tianhua et al. (2008). "Research on lateral stiffness of cold-formed steel composite wall." Journal of Chongqing University of Architecture (02): 75-79.
10. Shao Dayu and Hao Jiping (2017). "Finite element analysis of shear performance of sprayed lightweight mortar-cold-formed thin-walled steel composite wall." Steel structure 32 (12) : 1-6 + 21.
11. Wu Shiying. "Code for seismic test methods of buildings" (JGJ101-96) Introduction [J].Engineering seismic, 1997 (04) : 1-3.
12. Zhang Enyuan (2021). Research on seismic performance of new light steel-paper straw board composite wall, Northeast Forestry University. Master: 81.
13. Zhang Xiuhua and Zhang Enyuan et al. (2021). "Axial compression performance of cold-formed thin-walled square steel tube-straw board composite wall." Science and Technology and Engineering 21 (01): 283-289.
14. Zhou Tianhua and Shi Yu et al. (2006). "Experimental study on shear capacity of cold-formed steel composite wall." Journal of Xi 'an University of Architecture and Technology (Natural Science Edition) (01) : 83-88.